Geophysical Research Letters

Supporting Information for

Majority of Southern Ocean seasonal sea ice bloom net community production precedes total ice retreat

Shannon McClish* and Seth M. Bushinsky

Department of Oceanography, School of Ocean and Earth Science and Technology, University of Hawai‘i at Mānoa, Honolulu, HI

Contents of this file

Text S1. Float Data

Water column biogeochemical measurements of under-ice and recently ice-free waters are from profiling floats deployed through the Southern Ocean Carbon and Climate Observation and Modeling (SOCCOM) project (Johnson, Plant, Coletti, et al., 2017) (May 2021 data snapshot). Quality controlled data from float conductivity-temperature-depth (CTD), chlorophyll fluorescence, pH, particulate backscatter, nitrate, and oxygen sensors were used and detailed quality control and processing methods are described in (Johnson, Plant, Coletti, et al., 2017; Maurer et al., 2021). Reported chlorophyll concentrations are derived from float fluorescence measurements corrected for non-photochemical quenching and adjusted based on an empirical fit to high-performance liquid chromatography (HPLC) measurements from samples taken during SOCCOM float deployments (Johnson, Plant, Coletti, et al., 2017).

Phytoplankton carbon is derived from float measured particulate backscatter ($b_{bp}(700)$):

$$POC = 3.12 \times 10^4 \ (\pm 2.47 \times 10^3) \times b_{bp}(700) + 3.0 \ (\pm 6.8) \qquad (1)$$

$$C_P = 0.19 \times POC \pm 8.7, \quad (2)$$

where POC is particulate organic carbon (mg C m^{-3}) (Haëntjens et al., 2017; Johnson, Plant, Coletti, et al., 2017) and C_P is phytoplankton carbon (mg C m^{-3}) (Graff et al., 2015).

Float data spans from July 2015 to March 2021, totaling 64 float years from 31 floats, and is broadly distributed throughout the Southern Ocean from approximately 55°S to 70°S (Fig. 1, Table S1). Any float timeseries that had more than one consecutive missing profile during the winter to summer period for any of the variables was removed from analysis.

Text S2. Light and Sea Ice Concentration

Float position estimates during the winter when the float remains under ice are linear interpolations between the last profile prior to sea ice cover and the first profile post sea ice retreat. Sea ice concentration (SIC) from NSDIC/NOAA Climate Data Record of Passive Microwave Sea Ice Concentration (Meier, 2021) and incident shortwave radiative flux from the ERA5 reanalysis (Hersbach et al., 2020) were matched to interpolated float tracks. Float data was included in the analysis if the float was under ice with satellite SIC >80% for at least one month of the year and if both the winter nitrate maximum and spring nitrate minimum were observed. After sea ice breakup, SIC is used to determine day of total sea ice retreat, defined herein as the first day of sea ice free conditions at the float location. One float season (WMO 5904859, 2017-18) never reaches 0% SIC, so the sea ice minimum day is used instead. Mixed layer depth is calculated based on a density threshold of 0.03 kg m^{-3} from 10 m or the shallowest measured depth for under-ice floats following (de Boyer Montégut, 2004). Mixed layer median light (I_g) is estimated as:

$$I_g = I_0 e^{-K_{PAR} \cdot \frac{MLD}{2}}, \quad (3)$$

where PAR at the surface (I_0) is estimated from 2.3*incident shortwave radiative flux at the surface (Britton & Dodd, 1976; Westberry et al., 2008). The diffuse attenuation coefficient of PAR (K_{PAR}) was estimated from (Morel et al., 2007):

$$K_{PAR} = 0.0864 + 0.884 \times K_{490} - 0.00137 \times {K_{490}}^{-1}, \text{ when MLD} \leq (K_{490})^{-1} \text{ m}^{-1} \quad (4)$$

$$K_{PAR} = 0.0665 + 0.874 \times K_{490} - 0.00121 \times {K_{490}}^{-1}, \text{ when MLD} > (K_{490})^{-1} \text{ m}^{-1}, \quad (5)$$

where K_{490}, the diffuse attenuation coefficient at 490nm, was derived from float estimated chlorophyll following (Morel et al., 2007):

$$K_{490} = 0.0166 + 0.0742\ Chl^{0.68955}. \quad (6)$$

I_g is adjusted for sea ice cover assuming a 10% transmittance through sea ice which falls within the range of available Southern Ocean transmittance observations (Castellani et al., 2020)

Text S3. Calculation of tracer timing thresholds

Float data were interpolated to a uniform daily timestep and 1m depth grid. Mixed layer property means, mixed layer depth, and depth integrated nitrate were smoothed with a 30-day running average. Nitrate was normalized to salinity to avoid sea ice melt biasing seasonal changes in nitrate due to biological processes, though this is a small adjustment (Papadimitriou et al., 2012).

The timing of the start of salinity decreases due to melt is identified as the day mixed layer salinity decreases by 0.015 from the winter maximum and continues to decrease to the minimum in spring. The satellite SIC threshold is identified when satellite SIC decreases by 2.5% from its maximum. The 0.015 salinity threshold was chosen to be comparable to the SIC threshold based on the mean slope of the linear regressions of satellite SIC and mixed layer mean salinity for each float as SIC decreases to 60% (Fig. S2, SIC vs mixed layer salinity).

The timing of initial sea ice breakup is estimated as the average of the three dates of mixed layer oxygen increase past threshold, mixed layer salinity decrease past threshold, and float matched SIC decrease past the threshold. Oxygen concentrations are strongly influenced by sea ice cover, which limits the exchange between the surface ocean and atmosphere, such that upwelled deep waters that are low in oxygen remain strongly undersaturated in the winter during maximum sea ice cover. Differences in sea ice breakup timing and melt estimated from salinity, satellite-derived SIC, or oxygen can be due to the uncertainty of float position under ice affecting satellite SIC to float matchups, uncertainties in satellite-derived SIC, a potential decoupling of freshening and sea ice cover due to melting and advection of sea ice, or increases in oxygen concentrations due to horizontal gradients and advection. However, there is good agreement between the timing of mixed layer oxygen increase, salinity decrease, and a decrease in sea ice concentration on the seasonal timescale of interest (Fig. S1). Estimating initial sea ice breakup from the average of all three proxies is done to minimize the impact of the particular uncertainties for each individual proxy.

Start of nitrate drawdown is determined when mean mixed layer nitrate concentrations drop below the winter maximum (mean of two highest values) minus 0.2 μmol kg^{-1} [NO_3^-]. The oxygen threshold calculated from the 0.2 μmol kg^{-1} nitrate concentration multiplied by an O:N stoichiometric ratio of 154/17 (Hedges et al., 2002). This was repeated using the mean July (winter) O:N ratio observed for each float and no difference in timing was found. Changes in mixed layer oxygen and nitrate can arise due to vertical or horizontal advection, entrainment, photosynthesis, or respiration, while oxygen is additionally exchanged with the atmosphere. Setting the oxygen threshold from the nitrate threshold is done to evaluate if changes in oxygen are driven by biology,

and therefore accompanied by changes in nitrate, or decoupled from nitrate changes and due to openings in sea ice cover and exposure to the atmosphere.

Timing of seasonal changes in phytoplankton biomass is estimated by calculating phytoplankton growth initiation (GI). GI is defined as the point when the time derivative of either Chl or C_p exceeds the median time derivative computed for the growth period and has previously been used to infer bloom phenology in the Southern Ocean seasonal sea ice zone (Hague & Vichi, 2020). GI was calculated using both float-derived mean mixed layer and MLD integrated Chl and C_p concentrations to test for differences due to accumulation or dilution. GI estimates from the rate of change in depth integrated and mean mixed layer concentrations are similar for both chlorophyll and C_p, and we use GI estimated from mean mixed layer concentration in the analysis as the mixed layer is primarily shoaling during the winter to spring period of interest (Behrenfeld & Boss, 2018).

Growth initiation estimates occur by definition after the first occurrence of an increase in rates of change (bloom onset) used in previous SSIZ phenology studies (Arteaga et al., 2020; Uchida et al., 2019). Growth initiation was chosen over bloom onset because $d[C_{phyto}]/dt$ can be >0 throughout the winter, even though MLD integrated and mean mixed layer $[C_{phyto}]$ remains near zero and nitrate is stable or increasing, and is thus less suitable for discerning when phytoplankton production begins to significantly impact surface biogeochemistry.

Text S4. Net Community Production

Net community production was calculated from the seasonal drawdown of salinity-normalized nitrate integrated to the depth of the deepest winter mixed layer from the preceding winter. This integration depth is chosen to estimate the amount of carbon removed from surface in the spring that would not be re-entrained the following winter, and to include production occurring just below

the base of the mixed layer. Changes in in nitrate that result from vertical and horizontal advection or diffusion are not explicitly estimated due to difficulty in accurately parameterizing these fluxes under sea ice and thus introduce uncertainty into the NCP estimates. However, we estimated the contribution from these processes to be small compared to the magnitude of biological drawdown during this period, as described below. Estimating NCP to the base of the winter mixed layer avoids uncertainties arising from that sporadic mixing events below the spring/summer MLD not captured by the float 10-day sampling, and reduces the contribution of vertical advection because the winter mixed layer is deeper than estimates of Ekman depth in the SSIZ (Elipot & Gille, 2009). Bloom NCP is estimated from the maximum nitrate profile after the deepest winter mixing to the minimum nitrate profile that occur between July and the end of March for each float. On average, the MLD max occurs 54 days before a mixed layer nitrate decreases past the threshold, but for four bloom timeseries only (5906033-2020, 5374-2018, 5904855-2018, 5904468-2017), the maximum MLD occurs between 1-8 days after mixed layer nitrate concentrations decrease past the threshold, and so the absolute maximum winter value of nitrate is used as the start of the bNCP calculation instead. To assess potential uncertainties due to horizontal advection, we referenced the Biogeochemical Southern Ocean State Estimate (BSOSE) (Verdy & Mazloff, 2017) upper 150m nitrate budgets from [iteration 121, 2013-2016], which indicate horizontal advection is small (approximately 10-15%) compared to the biological signal during the productive season (not shown, available online at http://sose.ucsd.edu/). BSOSE assimilates observations from biogeochemical floats, shipboard data, and satellites estimates and maintains closed budgets to provide an estimate of Southern Ocean biogeochemistry, physics, and sea ice state which has been extensively validated. While individual float data-model misfits do exist, we reference only the effect of advective processes on nitrate within the model. Furthermore, the NCP estimates in this

study are of a similar magnitude as NCP from previous in-situ studies using a variety of different methods (Arteaga et al., 2019; Briggs et al., 2018; Ishii et al., 2002; Johnson, Plant, Dunne, et al., 2017; Lin et al., 2021). Together, these comparisons give good confidence that the nitrate drawdown approach used in the present study are accurate estimates of bloom NCP. The reported p-values (two sided) and coefficients of determination were calculated with the SciPy stats pearsonr function**.**

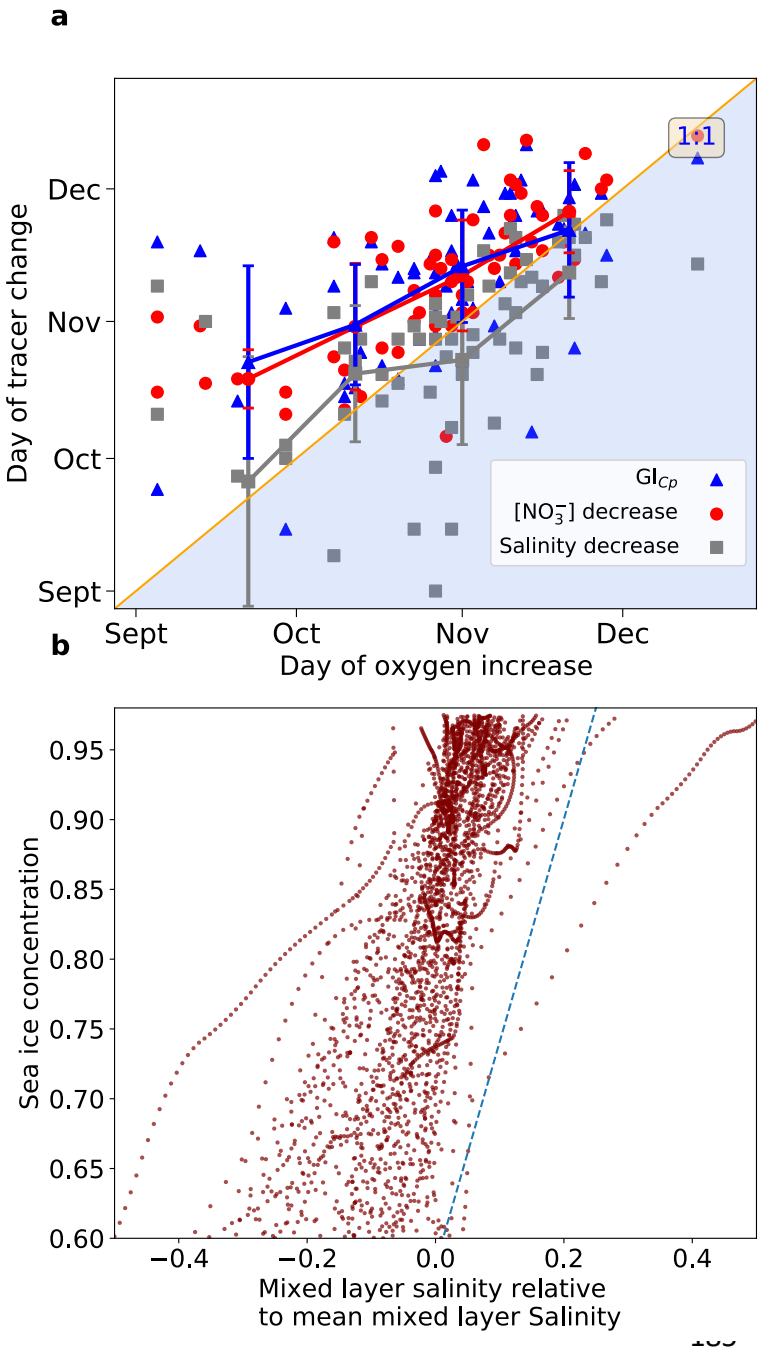

Figure S1. Rational for estimated timing of sea Ice break-up. A) Paper Figure 3 repeated with oxygen increase day instead of "Sea ice breakup day" on the x-axis and day of mean mixed layer nitrate decrease and GI_{Cp} vs float measured mean mixed layer salinity decrease day and on the y-axis. Twenty-day bin mean and standard deviations are shown by the error bars of the same color. Sea ice breakup used in analysis is the mean of the day of SIC decrease, day of salinity decrease and oxygen increase to indicate sea ice breakup. Oxygen increase and salinity decrease timing fall on or near the 1:1 line on average, while GICp and nitrate decrease follow (fall above 1:1 line) oxygen increase and salinity decrease.

B) Changes in mixed layer salinity relative to sea ice melt were assessed to determine comparable salinity and SIC thresholds. The mean mixed layer salinity (relative to mean salinity for clarity) is plotted vs satellite SIC during the period of initial SIC decrease to 60% SIC. The salinity threshold used in the analysis was determined from the mean slope of a linear regression line for each float mixed layer S vs. SIC which is 1.6 after outliers (25th and 75th quantiles) are removed. The mean slope used is indicated in the figure with the blue dashed line. This indicates an approx. ~.015 change in mixed layer salinity for the 2.5% SIC decrease threshold.

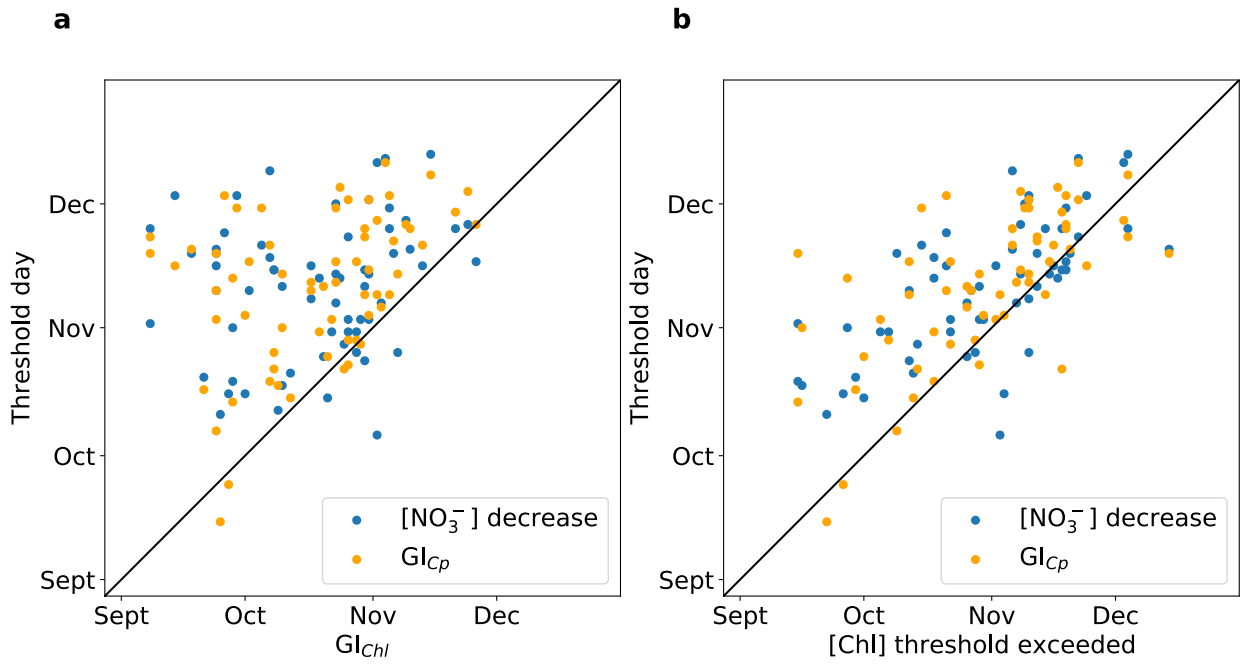

Figure S2. **Relationship between nitrate threshold and GI_{Cp} and two different chlorophyll-based growth initiation metrics**. a) Comparison of GI_{chl} vs timing of timing of nitrate decrease past the 0.2 µmol/kg threshold and GI_{Cp} (b) Comaprison of timing of chl exceeding 0.035mg/m^3 vs timing of nitrate decrease past 0.2 µmol/kg threshold and $GI_{Cp.}$ Estimation of growth intiation from the timing of an increase in the rate of mixed layer chlorphyll concentration was sensitive to small increases in chlorophyll (<.035mg/m^3) that were before an increase in Cp or nitrate concentration decrease, which both plot well above the 1:1 line on a). Earlier GI_{chl} was not consistent, but could occur months before, to within days of GI_{Cp} and nitrate decrease, making GI_{chl} not appropriate for determining when phytoplankton began to drawdown surface nutrients and carbon.

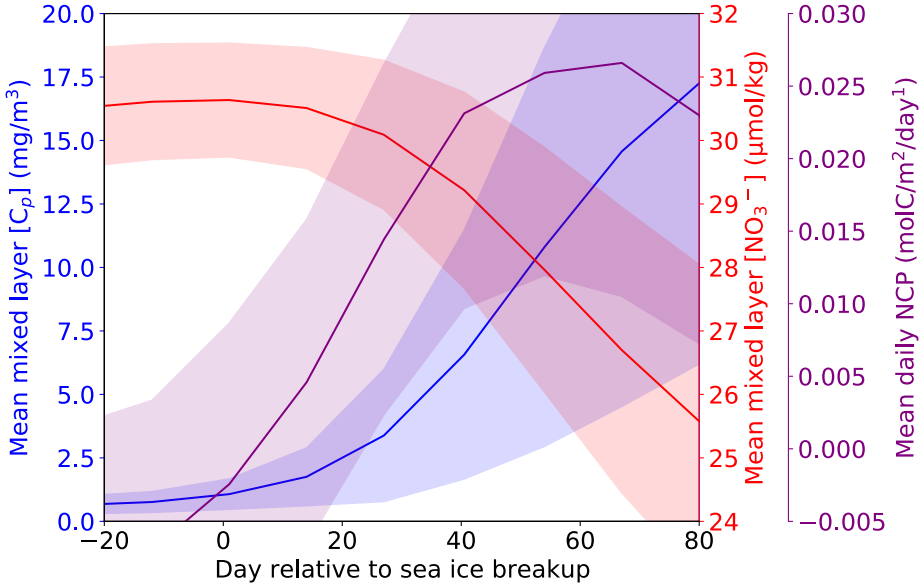

Figure S3. Comparison between temporal changes in mean mixed layer nitrate and C_{phyto} concentrations and daily NCP with respect to sea ice breakup. 10-day binned mean daily NCP (purple line), mean mixed layer nitrate (red line), mean mixed layer C-phyto (blue line) vs. day relative to sea ice breakup. Standard deviations shown by shaded area for each. Daily NCP > 0 after sea ice breakup, consistent with increases in phytoplankton carbon and mixed layer nitrate decrease.

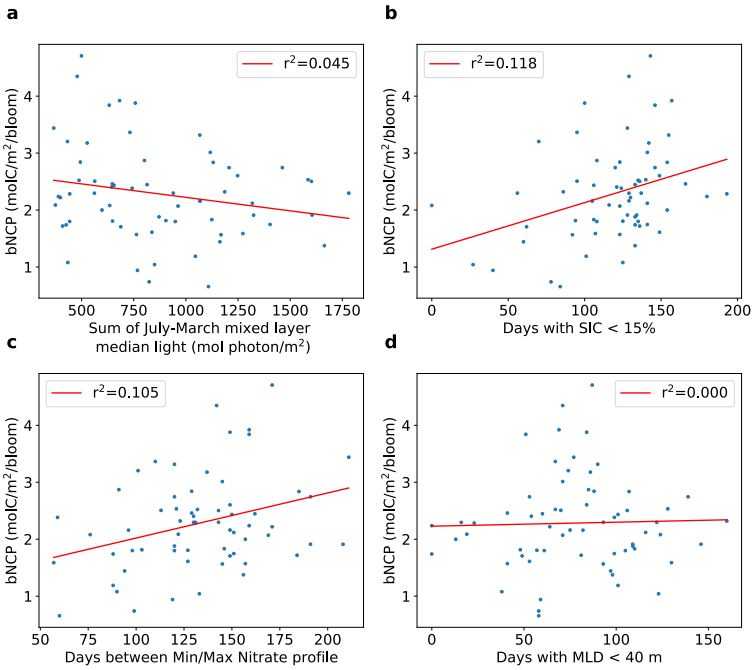

Figure S4. Light availability is not found to be primary factor influencing the magnitude of bNCP. Scatter plots and ordinary linear regression (red line) between bNCP and a) sum of mixed layer median light from July to end of March , b) days SIC < 15%, c) Days between min and max Nitrate profile (time over which bNCP is calculated), and d) days with a MLD <40m. The

respective *P*-values are a).091 b) .005, c).009, d) .817. bNCP shows a weak but significant relationship with the number of days with SIC < 15%, but this is confounded by the fact that earlier sea ice retreat will by definition lead to more days with SIC <15%. If this relationship were equal to or stronger than the bNCP vs. Sea ice breakup day (Fig. 5) it could have indicated that the primary factor controlling bNCP was duration of open water; however, this does not appear to be the case.

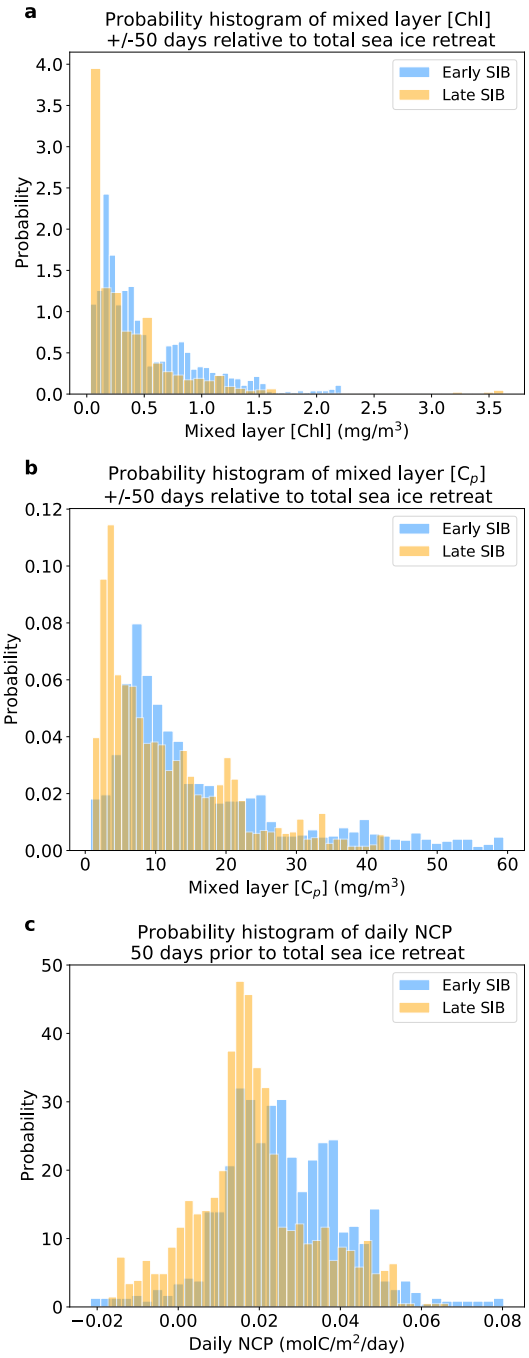

Figure S5. Higher daily NCP prior to total sea ice retreat and overall higher later winter/spring mixed layer chlorophyll and C_{phyto} concentrations for floats that observe early vs. late sea ice breakup. A) Daily NCP rates comparing occurrences of early (blue) and late (gold) sea ice breakup in the 50 days before complete sea ice retreat (open water day). B) Mean mixed layer chlorophyll and C) phytoplankton carbon (right) concentrations for the 50 days before and after open water day comparing early vs late SIB occurrences.

Table S1. WMO Float ID, year, mean float-season locations, bNCP, fraction bNCP before total sea ice retreat, and tracer timings for all float seasons analyzed.

Float WMO	Year[1]	Mean Latitude during bloom (°N)	Mean Longitude during bloom (°E)	Oxygen threshold (year day)	Sea Ice Breakup (year day)	Salinity threshold (year day)	Oxygen threshold (year day)	GI_{Cp} (year day)	GI_{Chl} (year day)	bNCP (mol C m^{-2} $bloom^{-1}$)
5904180	2015	-65.4	203.8	248	259	313	306	323	251	2.3
5904180	2016	-64.5	206.1	285	272.7	296	293	290	264	1.6
5904397	2015	-61.6	344.9	314	314.7	316	329	327	251	1.6
5904397	2016	-60.4	128.8	320	297.3	298	321	330	330	2.3
5904397	2017	-61.8	247.1	297	292	301	307	301	302	2
5904397	2018	-60.4	351.7	320	314.3	313	329	313	309	1.7
5904467	2015	-61	4.2	318	310	315	323	280	267	1.1
5904467	2016	-62.3	352.8	303	292	281	314	321	275	2.5
5904467	2017	-59.9	352.3	272	268	274	284	258	268	2.2
5904468	2015	-64.5	3.1	299	295.3	289	318	319	304	2.5
5904468	2016	-66.1	4.2	272	277.3	277	289	308	274	3
5904468	2017	-64.8	37.7	257	265.7	305	291	305	283	3.8
5904468	2018	-64.6	2.1	310	305	313	320	325	317	3.2
5904471	2015	-65.9	2.2	293	304.3	291	322	292	280	2.8
5904471	2016	-65.1	2.8	300	290	272	311	316	296	2.7
5904471	2017	-64.7	5.6	263	256.3	270	292	287	271	3.9
5904471	2018	-67.1	5.4	312	301	301	320	314	290	2.4
5904472	2015	-68.5	345.9	315	305.3	299	324	329	314	1.8
5904472	2016	-69.1	338.7	311	298.7	282	317	304	292	2.9
5904472	2017	-69.2	330.1	315	309.3	307	336	336	304	1.2

5904472	2018	-66.7	318.4	309	318.3	321	345	331	306	0.7
5904855	2018	-68.7	274.8	302	292.3	297	279	313	306	2.7
5904855	2019	-68.9	277	315	321.7	324	318	321	296	1.8
5904859	2017	-70.1	257.3	349	330	318	347	342	319	2.1
5905075	2017	-68.1	255.1	296	280.3	304	305	317	271	2.2
5905075	2018	-69.9	260.1	319	316.3	293	331	330	313	1
5905077	2017	-65.7	254.9	283	285.3	284	294	288	285	2.3
5905078	2017	-66.7	235.1	300	315.7	309	330	338	328	2.5
5905080	2018	-68.1	263.7	303	280	258	304	307	295	1.9
5905080	2019	-67.3	281	248	278.3	284	289	267	270	2.6
5905100	2017	-65.4	167.3	286	270.3	301	288	298	294	3.4
5905100	2018	-65	164.8	300	277.3	244	301	295	298	2.2
5905102	2017	-69.8	172.5	324	328.3	329	323	326	310	1.7
5905374	2018	-64.2	141.9	293	294	301	298	315	293	2.5
5905635	2018	-67.1	190	306	296.3	311	314	314	267	1.8
5905635	2019	-66.4	191	305	309.3	293	311	310	307	1.7
5905636	2018	-67	210.5	304	300.7	306	315	318	283	1.8
5905636	2019	-66.9	210.6	325	328.3	324	329	333	325	2.1
5905636	2020	-67	210.7	332	324.3	328	337	320	257	2.1
5905637	2018	-71.4	204.1	331	311	314	335	334	296	1.4
5905637	2019	-71.3	190.1	326	331.7	327	327	336	299	2.3
5905637	2020	-69	190.7	323	314	323	315	327	303	3.2
5905638	2018	-68.4	174.1	328	325.7	324	343	325	280	0.7
5905638	2019	-69.1	172.2	326	330	320	319	299	281	0.9
5905639	2018	-67.3	236.2	313	294.3	309	325	334	278	2.4
5905991	2019	-61.7	323.2	290	290.7	287	319	295	281	1.9
5905991	2020	-59.2	325.7	281	250.3	252	297	313	303	4.7
5905992	2019	-65.9	330.4	300	300	301	320	307	267	1.7
5905992	2020	-64.6	330.4	303	302.7	301	319	329	303	3.4

5905994	2019	-65.2	320.3	301	311	305	317	339	297	3.9
5905994	2020	-64.4	323.8	317	315.7	319	346	345	308	2.2
5905995	2019	-67	342	314	322	326	337	334	272	1.6
5905995	2020	-67.6	338.6	316	315.7	314	334	337	309	1.6
5905997	2019	-64.4	119.6	230	267.7	277	299	302	301	2.4
5905997	2020	-63.9	117.1	300	284.3	306	304	302	299	1.8
5905998	2020	-63.7	123.8	283	288.7	299	285	291	282	2.5
5906000	2019	-63.5	100.2	256	264	218	304	321	301	2.3
5906005	2019	-59.7	329.3	305	297.7	296	307	296	299	3.3
5906005	2020	-59.6	330.4	296	273.7	258	312	316	290	4.3
5906006	2019	-58.6	339.1	307	304	302	307	308	304	2.8
5906033	2019	-66.5	22.4	288	303.3	314	324	323	267	1.9
5906033	2020	-66.8	0	307	303.7	298	328	337	269	2.4
5906034	2019	-63	28.5	290	290.7	293	299	318	311	2.1
5906034	2020	-64.1	28	281	295.3	307	323	324	261	1.4

[1]Year corresponds to the winter/spring year for each bloom period.